AGU PUBLICATIONS

JGR

Journal of Geophysical Research: Atmospheres

RESEARCH ARTICLE
10.1002/2013JD020611

Key Points:
- Interpolation of daily rainfall data using 15 spatial interpolation methods
- Relative skill of interpolation techniques depends on observation density
- High and low rainfall events should be treated with different techniques

Correspondence to:
C. Camera,
c.camera@cyi.ac.cy

Citation:
Camera, C., A. Bruggeman, P. Hadjinicolaou, S. Pashiardis, and M. A. Lange (2014), Evaluation of interpolation techniques for the creation of gridded daily precipitation (1×1 km^2); Cyprus, 1980–2010, *J. Geophys. Res. Atmos.*, *119*, 693–712, doi:10.1002/2013JD020611.

Received 22 JUL 2013
Accepted 17 DEC 2013
Accepted article online 20 DEC 2013
Published online 31 JAN 2014

Evaluation of interpolation techniques for the creation of gridded daily precipitation (1×1 km^2); Cyprus, 1980–2010

Corrado Camera[1], Adriana Bruggeman[1], Panos Hadjinicolaou[1], Stelios Pashiardis[2], and Manfred A. Lange[1]

[1]Energy, Environment, and Water Research, Cyprus Institute, Nicosia, Cyprus, [2]Cyprus Meteorological Service, Nicosia, Cyprus

Abstract High-resolution gridded daily data sets are essential for natural resource management and the analyses of climate changes and their effects. This study aims to evaluate the performance of 15 simple or complex interpolation techniques in reproducing daily precipitation at a resolution of 1 km^2 over topographically complex areas. Methods are tested considering two different sets of observation densities and different rainfall amounts. We used rainfall data that were recorded at 74 and 145 observational stations, respectively, spread over the 5760 km^2 of the Republic of Cyprus, in the Eastern Mediterranean. Regression analyses utilizing geographical copredictors and neighboring interpolation techniques were evaluated both in isolation and combined. Linear multiple regression (LMR) and geographically weighted regression methods (GWR) were tested. These included a step-wise selection of covariables, as well as inverse distance weighting (IDW), kriging, and 3D-thin plate splines (TPS). The relative rank of the different techniques changes with different station density and rainfall amounts. Our results indicate that TPS performs well for low station density and large-scale events and also when coupled with regression models. It performs poorly for high station density. The opposite is observed when using IDW. Simple IDW performs best for local events, while a combination of step-wise GWR and IDW proves to be the best method for large-scale events and high station density. This study indicates that the use of step-wise regression with a variable set of geographic parameters can improve the interpolation of large-scale events because it facilitates the representation of local climate dynamics.

1. Introduction

Precipitation does not take place continuously, neither spatially nor temporarily. While monthly data or long-term averages can be interpolated quite easily over a given area due to their smooth characteristics, this is more complex when considering daily precipitation values. As pointed out by *Hofstra et al*. [2008], there are many studies that compare different interpolation techniques for long-term means, or monthly and annual values, but there are few that address the interpolation of daily data. One of the main risks, when considering daily data, lies in the possibility of partly reducing the variability of the original data and to lose local relative peaks of precipitation [*Shen et al*., 2001].

Daily gridded data sets of meteorological variables, precipitation in particular, are very useful for many applications. The increasing number of global and regional climate modeling experiments calls for reliable observational data sets to evaluate and verify model outputs [e.g., *Fundel et al*., 2010; *Maraun et al*., 2012]. Such data sets are also instrumental to assess the influence and relevance of climate change over a certain area [e.g., *Barnett et al*., 2005]. Climate change impact studies need climate information and climate projections at high spatial resolution (~ 1 km). This is significantly higher than what current state-of-the-art models can offer (10–25 km). Gridded data at ~ 1 km resolution are also most useful for hydrological studies, e.g., to validate spatial rainfall or weather generator outputs [e.g., *Kilsby et al*., 2007], and to serve as input to distributed hydrological models [e.g., *Gosling and Arnell*, 2011; *Parkes et al*., 2013]. Moreover, they can be used for water resources analyses [e.g., *Kizza et al*., 2012] and water management applications, which are often related to agricultural activities [e.g., *Fader et al*., 2010; *Supit et al*., 2012]. Other fields that will benefit from gridded data sets include investigations on biodiversity loss and terrestrial ecosystem studies [e.g., *Gritti et al*., 2006; *Avellan et al*., 2012].

Frequently used techniques applied to interpolate monthly and annual precipitation data are regression models [e.g., *Ninyerola et al*., 2000; *Vicente-Serrano et al*., 2003], inverse distance weighting (IDW) [e.g., *Perry and Hollis*, 2005], angular distance weighting (ADW) [e.g., *Kiktev et al*., 2003], and kriging (KR) [e.g., *Goovaerts*, 2000]. Thin plate splines (TPS) have been tested on precipitation data [e.g., *Vicente-Serrano et al*., 2003] but their tendency to oversmooth the calculated surfaces leads them to return better results when interpolating temperature [e.g., *Jarvis and Stuart*, 2001]. In general, these techniques are singularly applied, but there are also studies that use a combination of various methods [*Agnew and Palutikof*, 2000; *Vicente-Serrano et al*., 2003]. In most cases, the combination of techniques is motivated by an attempt to remove the effects of certain geographical characteristics (e.g., elevation, distance from the coast, spatial location, etc.). *Perry and Hollis* [2005] explained that this can be either done through a normalization of the values of interest with respect to a long-term average or through the definition of a regression model based on geographical variables.

The paucity of studies on the interpolation of daily meteorological data results also in a lack of a systematic work that compares and evaluates, at this temporal resolution, the skill of different interpolation techniques. Exceptions are the two combined studies by *Hofstra et al*. [2008] and *Haylock et al*. [2008]. The latter study is utilized for very large scales (all Europe) and therefore targets a very different spatial resolution. Another study targeting large scales (all Asia) is that by *Yatagay et al*. [2012]. They are producing a database (APHRODITE) that includes daily precipitation and monthly climatology gridded data. However, the main focus of their study is the development of an algorithm for interpolation, including also an extended quality control of input data. They used an angular distance weighting scheme as in *Willmott et al*. [1985] and did not evaluate different interpolation techniques. Other studies in which a daily gridded data set is constructed are those of *Frei and Schär* [1998] and *Perry et al*. [2009]. In both studies, the interpolation technique (angular and inverse distance weighting, respectively) is selected because of its simplicity. Comparisons of different spatial interpolation techniques have been made by *Bussières and Hogg* [1989] for daily precipitation in the Great Lakes Region in North America, by *Brown and Comrie* [2002] for mean winter temperature and precipitation in Arizona and New Mexico (USA), and by *Weber and Englund* [1992] for contaminant concentrations. *Perry et al*. [2009] used, based on the interpolation of monthly data [*Perry and Hollis*, 2005], also the coupling of regression with inverse distance weighting, recognizing a certain number of geographical covariables (easting and northing, elevation, proximity to water bodies, and proximity to urban areas) as possible predictors for different climatic variables (e.g., precipitation, temperature, wind speed, sunshine, and vapor pressure). However, an in-depth discussion of the reasons leading to the selection of covariables was not presented. Other studies that evaluate daily precipitation are those of *Carrera-Hernandez and Gaskin* [2007] and *Symeonakis et al*. [2009], but these authors focussed on geostatistical techniques, only. *Herrera et al*. [2012] also applied kriging to develop a 50 year gridded data set over Spain, but the spatial resolution of their study was quite coarse (~ 20 km).

Geographically weighted regression (GWR) is increasingly used to model climatic variables [e.g., *Brunsdon et al*., 1996; *Fotheringham et al*., 2002]. *Szymanowski and Kryza* [2012] found that GWR performed better than linear multiple regression (LMR) for the modeling of temperature at different time scales, including daily. To create their final data set, they coupled GWR with kriging. Another example is that of *Bostan et al*. [2012], who applied GWR to estimate the spatial distribution of average annual rainfall over Turkey, and compared it to other techniques such as LMR and different types of kriging. For their case study, GWR performed better than LMR, but universal kriging was recognized as the best overall method.

The aim of this study is to provide a complete overview of the performance of 15 interpolation techniques for the gridding of daily precipitation over a topographical complex area. The techniques are evaluated through a system of scores, using an approach very similar to *Vicente-Serrano et al*. [2003] and *Hofstra et al*. [2008]. An analysis of the performance of the various techniques due to different rainfall amounts, different topographical attributes, and different observation density is included. The spatial resolution selected for the output maps is 1×1 km^2.

The Republic of Cyprus (Figure 1) serves as the study area for this analysis. The area is not large but it has a very complex topography, which has a strong effect on the rainfall distribution. Annual average rainfall ranges from about 1100 mm in the higher mountainous area to around 300 mm in the plains of the central eastern part of the island [*Michaelides et al*., 2009]. Rainfall is not only highly variable in space but also in time, with a well defined annual cycle with wet months between November and March and almost completely dry

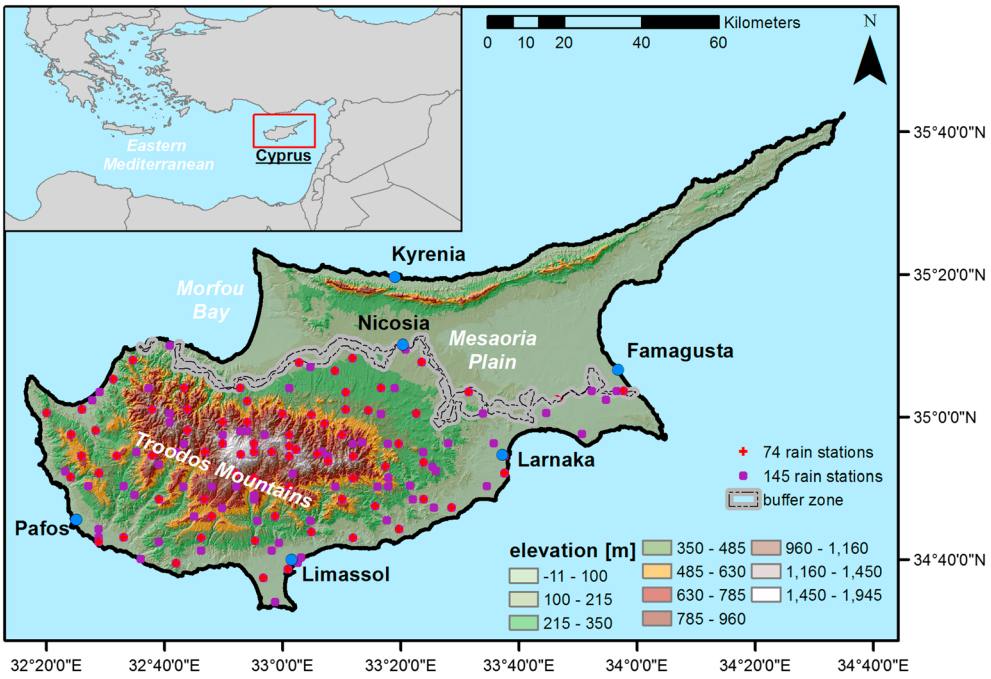

Figure 1. The island of Cyprus with its main political and geographical characteristics and the locations of the 74 and 145 precipitation stations used in this study. The study area covers the area under the effective control of the government of the Republic of Cyprus (south of the buffer zone), including the British Bases.

summers [*Hadjinicolaou et al.*, 2011]. Cyprus, therefore, provides an opportunity to analyze very different rainfall regimes, covering a large number of event types that may also occur in different areas around the world. Thus, our results are not restricted to the island of Cyprus, but provide insights on much larger, regional scales.

The following sections present a brief introduction to the main geographical and meteorological characteristics of Cyprus, followed by a complete overview of the methods applied. The two data sets used are presented and attention is given to the description of both the interpolation methods and the setup of the ranking system to evaluate and compare their performance. In section 4, the results are presented and discussed, followed by a concise summary and conclusions.

2. Study Area

Cyprus is an Eastern-Mediterranean island, located between 34–36°N and 32–35°E. It has two mountain chains, the Troodos, located in the central-west part of the island with its highest peak, Mount Olympus, reaching 1951 m a.s.l., and the Kyrenia Range, which runs for 160 km parallel to the northern coast of the island reaching a maximum elevation of 1024 m a.s.l. at Mount Kyparissovouno. The Mesaoria Plain, which is the main agricultural area of the country, is nestled between the two mountain ranges. The island has been politically divided since the Turkish invasion of 1974. This study analyzes the precipitation over the area currently controlled by the Republic of Cyprus, which covers the southern part of the island (Figure 1).

Precipitation in Cyprus is concentrated in the period between October and May, across two different solar years. December, January, and February are the wettest months, while October–November and March–April–May are transitional months. Specifically, October and March can experience very different rainfall conditions, ranging from 0 to more than 100 mm of cumulated rainfall. Between June and September, rainfall events are very rare and in some years completely absent.

During all four seasons precipitation is highest on the Troodos Mountains (Figure 2). However, during the Autumn-Winter period precipitation is more abundant on the western flank of the mountains, while during the Spring-Summer period it is more abundant in the Mesaoria plain, on the eastern side of the mountains.

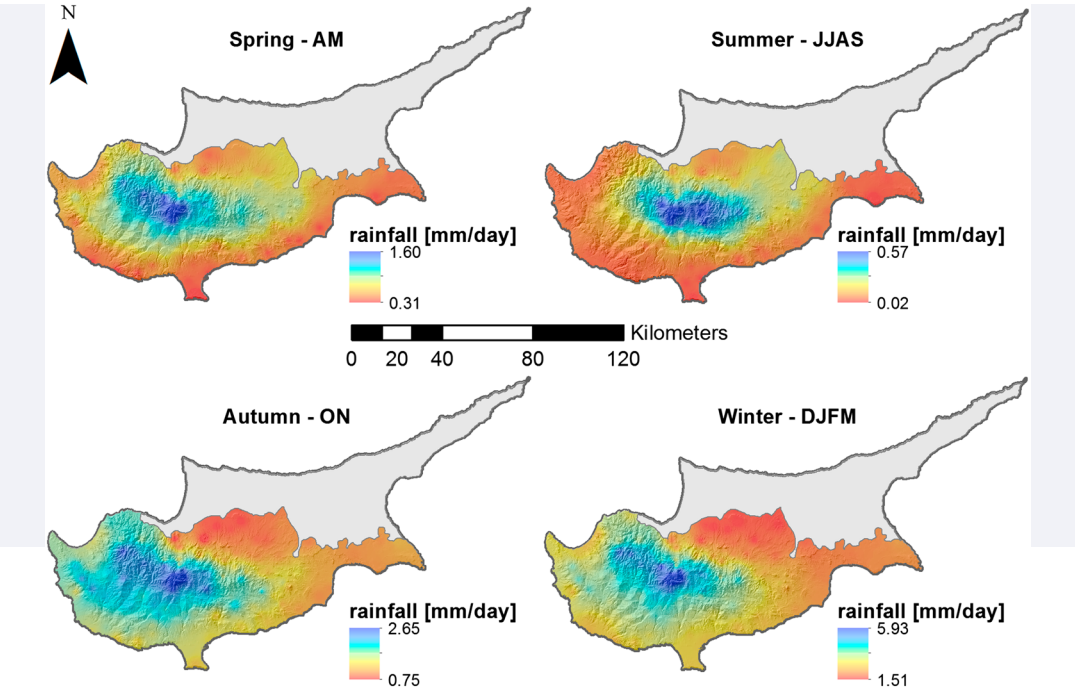

Figure 2. Daily average rainfall for seasons for the period 1980–2010. AM is April and May; JJAS is June, July, August, and September; ON is October and November; DJFM is December, January, February, and March. The maps were obtained with a simple inverse distance weighting (IDW) interpolation of the data registered at the 145 stations.

This seasonal difference is related to different meteorological processes that lead to the onset of a precipitation event. During Autumn-Winter most of the precipitation is due to humid fronts arriving from the west. These humid fronts enter the island along the south-western coast and experience two different effects. The first is a land-sea effect, due to a different temperature between the sea and the earth, which can trigger vertical movements of air masses and facilitate the onset of a precipitation event. The second effect is a topographical effect. Moving east, the humid front meets the foothills of the Troodos Mountains, so that the air masses are pushed upward and create additional rainfall events. On the other hand, the Troodos Mountains also act as a barrier for these currents, therefore concentrating rainfall on their western side. The result is a maximum of precipitation aligned along the main ridge of the mountains and a relatively higher abundance of rain on the western flanks, compared to the eastern flanks at the lee side ("rain-shadow"). During Spring-Summer, convective events originate directly on the Troodos Mountains and, in this case, the predominantly west-east winds push the rainfalls toward the Mesaoria Plain and Nicosia, sparing the south-western and west coast [*Michaelides et al*., 2008].

3. Methods

In the present study, different regression models and interpolation techniques are tested and evaluated, both singularly and combined, on daily rainfall data. The combination methods apply a regression model, followed by the interpolation of the residuals and the subsequent summation of the two contributions. This methodology allows the selection of geographical variables for regression, focusing the attention on the physical processes and on the climatology that dominates the precipitation events over the area of interest. Normalization of the data with respect to a long-term average was not used because the long-term average values are not representative of the highly variable daily processes.

3.1. Data Acquisition and Quality Control

The first part of the work involved the creation and the quality control of the data set to be used in the following interpolation phase. The base of the work was represented by daily rainfall time series made available by the Cyprus Meteorological Service (CMS). The initial database was made up of time series recorded at

Table 1. Summary of Interpolation and Regression Methods Used

Abbreviation	Full Name	R Library	Key References
LMR	linear multiple regression	stats	
GWR	geographically weighted regression	spgwr	*Brunsdon et al.* [1996]; *Fotheringham et al.* [2002]
SWLMR	stepwise linear multiple regression	stats	*Akaike* [1970]
SWGWR	stepwise geographically weighted regression	stats, spgwr	
IDW	inverse distance weighting	gstat	*Shepard* [1968, 1984]
KR	Ordinary kriging	gstat	*Krige* [1951, 1966]; *Matheron* [1963]
TPS	3D thin plate sp-lines	fields	*Wahba and Wendelberger* [1980]; *Hutchinson* [1991]
LMR-IDW	linear multiple regression + IDW on residuals	stats, gstat	
LMR-TPS	linear multiple regression + TPS on residuals	stats, fields	
GWR-IDW	geographically weighted regression + IDW on residuals	spgwr, gstats	
GWR-TPS	geographically weighted regression + TPS on residuals	spgwr, fields	
SWLMR-IDW	stepwise linear multiple regression + IDW on residuals	stats, gstat	
SWLMR-TPS	stepwise linear multiple regression + TPS on residuals	stats, fields	
SWGWR-IDW	stepwise geographically weighted regression + IDW on residuals	stats, spgwr, gstat	
SWGWR-TPS	stepwise geographically weighted regression + TPS on residuals	stats, spgwr, fields	

74 stations used in a study by *Bruggeman et al.* [2011]. A second set included 145 stations (Figure 1), increasing the density of stations above all in the southern foothills of the Troodos Mountains and in the plain area in the south-east of the country.

The time series were tested for homogeneity considering both daily and monthly time lag. For the homogeneity test, the RHtestV3 software [*Wang et al.*, 2010; *Wang and Feng*, 2010] was used. At first, the monthly data were tested and statistically significant break points recognized. The RHtestV3 software allows the user to subsequently check if the monthly breaks have a corresponding break in the daily series.

3.2. Introduction to Interpolation Techniques

The several simple and combined interpolation techniques tested are summarized in Table 1. All regressions and interpolations as well as their evaluation were conducted in the R environment [http://www.r-project.org], where specific libraries such as gstat [*Pebesma*, 2004], fields [*Nychka et al.*, 2006], and spgwr [*Bivand and Yu*, 2013] enable interpolation with the selected techniques. For the regression models, a different equation is developed for each day.

3.3. Definition of the Geographical Variables for Regression

Six geographical variables were selected to represent the various climatological patterns and processes described in section 2 (Figure 3):

1. Elevation, to consider the orographic effect;
2. Distance to coast, to consider the land-sea effect;
3. East coordinate, to consider a general spatial pattern;
4. North coordinate, to consider a general spatial pattern too;
5. Distance from the main mountain ridge to the east, to consider the mountain shadow effect;
6. Distance from the main mountain ridge to the west, to consider the mountain shadow effect, too.

The last two variables are included to take into account the mountain shadow effect and the different behavior of precipitation in the wet and dry seasons. These two variables could appear correlated, but they allow the representation of the decrease of rainfall from the core of the mountain chain to the plains, which is expected to be different on the two sides of the mountains.

3.4. Regression and Interpolation Methods

A brief overview on the main characteristics of the simple methods is given in this section.

LMR: the approach is identical to simple least squares regression with a dependent and an independent variable. For simple regressions, the dependent variable is plotted against the independent one in a simple Cartesian plane and the straight line that minimizes the squared error is searched. Working with more than one independent variable, the process is exactly the same, only the workspace is more complicated than a simple two axes Cartesian plane.

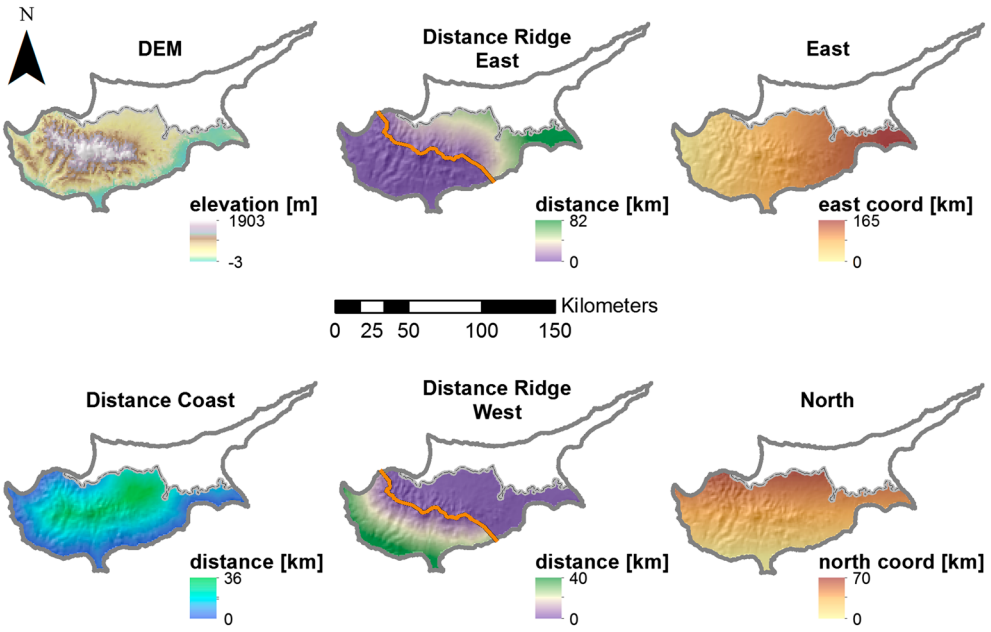

Figure 3. The six different geographical variables used for regression. All maps have the same resolution as the resulting daily precipitation maps (1×1 km^2). The North and East coordinates used for regression are those of the UTM (zone 36N) projection system (expressed in meters).

GWR: the method was presented by *Brunsdon et al*. [1996] and later improved by *Fotheringham et al*. [2002]. Its main difference with respect to linear multiple regression is that it does not fit a single regression model over the entire area of interest, but it searches for geographical differences. It means that the selected independent variables are the same, but their absolute and relative importance in the definition of the dependent variable can change over the study area, from location to location. In other words, if the linear multiple regression method implies a spatial stationarity, the geographically weighted regression does not. This nonstationarity is reached by fitting, in each point, the regression line on a limited number of observations and weighting each observation with respect to its distance to the point of interest. The number of observations to be included is selected on the base of a defined search radius, which can be set by the user or defined in each point by an automatic procedure [*Charlton and Fotheringham*, 2009], based on the minimization of the corrected Akaike Information Criterion (AIC_C) [*Hurvich et al*., 1998]. The search radius takes the name of bandwidth, while the distance weighting function is named kernel. In this study, the automatic definition of the bandwidth is adopted while the kernel is exponential [*Harris et al*., 2010].

SW: with a stepwise regression the aim is to evaluate which model is the best, in terms of accuracy and complexity. Starting with a regression model of N independent variables, variables are subtracted one by one, to achieve the best compromise between the accuracy of the prediction and the complexity of the model. The task can be carried out, similar to GWR, with the Akaike Information Criterion [AIC — *Akaike*, 1970]. Among different models, the lowest AIC value indicates the most parsimonious model in which the least information is lost. The AIC works only as a comparison between models and it is a relative measure; it is not an absolute indicator of how well a model reproduces the dependent variable. Stepwise regression was applied to both linear multiple regression and to geographically weighted regression.

IDW: this technique is based on the SYMAP algorithm of *Shepard* [1968, 1984]. It relates the unknown value of a certain variable in a defined point to the values of the same variable measured in other locations, on the base of the distance between the locations. The closer an observation is to the point of estimate, the higher its influence. This influence is expressed through a weight (w), which has the following formulation [*Shepard*, 1968]:

$$w_i(x) = \frac{1}{d(x, x_i)^p} \tag{1}$$

where x is the point where the estimate is wanted, x_i is one of the points where observations are available, d is the distance between the two locations, and p is an exponent that permits to give different forms to the

weighting function. The higher p is, the less importance is given to more remote observations. With the inverse distance weighting function used in this work (Table 1), it is also possible to include all observation points in the study area, or to limit the observation points either by means of a specified search radius or by selecting a precise number of known values. An exponent p equal to 2 was set, as default in the R function used, so not penalizing too much the contribution to the estimate of far away points. The number of observations used for each estimation was set to 12.

The only difference between IDW and angular distance weighting (ADW), which was not tested in this work, lies in how the weights are calculated. With ADW, the weights are computed based on the algorithm of *Shepard* [1968, 1984] and include the horizontal angles between the observations.

KR: as for regression and the distance weighting techniques, kriging creates an interpolated surface of the variable of interest, estimating its values where they are unknown on the base of observed neighboring data. The method was developed by *Krige* [1951, 1966] and *Matheron* [1963], and, as pointed out by *Hofstra et al*. [2008], it can be classified as a BLUE (best linear unbiased estimation) methodology. It means that in every point the estimation of the variable of interest is given by a linear combination of the neighboring observations, each weighted, and with the sum of weights equal to one. The weights are determined on the basis of a spatial covariance function describing the variability of the observations. This function is called variogram model and it is stationary; it is the same across the whole area of interest. The variogram model is defined and fitted based on an empirical variogram, which is calculated from the data. The empirical variogram can be not continuous and can result in a nonpositive definite matrix (it is an empirical covariance estimate); therefore, the fitting of a variogram model is necessary.

TPS: splines [*Wahba and Wendelberger*, 1980; *Hutchinson*, 1991], as kriging, are based on spatial covariance functions, and in fact often the two methods are compared and perform similarly [*Hutchinson*, 1993; *Laslett*, 1994]. The main difference lies in how the spatial covariance function is defined. Splines are in fact more flexible; the covariance function does not need to be estimated a priori, but what is estimated is "a smoothing parameter that determines an optimal balance between fidelity to the data and smoothness of the fitted spline function" [*Hutchinson*, 1995]. This author used a method that minimizes the generalized cross validation (GCV) to optimize the smoothing parameter.

3.5. Regression and Interpolation Models Evaluation

To compare the 15 different combinations of interpolation and regression techniques, an evaluation framework based on skill scores was set up. In this evaluation phase, a set of representative days was selected. Thiessen polygons were used to assign an area to every station and then the area-weighted average precipitation was calculated for every day. Rainy days, considered as days with an average precipitation over the study area greater than zero, were separated from nonrainy days, and the percentiles of the daily average precipitation were calculated for this data set. The final data set for the evaluation was restricted to 36 days, including a day with no rainfall, the day characterized by the minimum value of area average rainfall, the day with the maximum area average rainfall, and the 33 days in correspondence of the area average precipitation values representing the 3^{rd}, 6^{th}, 9^{th}, […], 99^{th} percentile. This set was constructed based on the 74 stations database and then used also for the 145 stations.

A cross-validation method was used to evaluate the different techniques. Considering N the number of stations (observations), each interpolation method was run N times for each day with $N-1$ training points and 1 test point. When using the step-wise regression, a single regression formula was calculated for each day and applied in the N runs. For each of the N runs, a different observation was used as test point, a gridded data set was created and the modeled value of the test location was extracted. Finally, the N modeled and observed values were compared with the help of the evaluation scores, presented below.

Second, four subsets were created from this set of representative days. These four subsets represented very low rainfall events (0^{th}–30^{th} percentiles — 12 days), low rainfall events (31^{st}–60^{th} percentiles — 10 days), medium-high rainfall events (61^{st}–84^{th} percentiles — 8 days), and high rainfall events (85^{th}–100^{th} percentiles — 6 days). The subdivision was made based on the cumulative distribution of all the area average daily rainfall values (Figure 4). The subsets, being calculated on area average values, do not only represent an increasing amount of rainfall, but also represent local (very low to medium high rainfall) and large-scale (high rainfall) events.

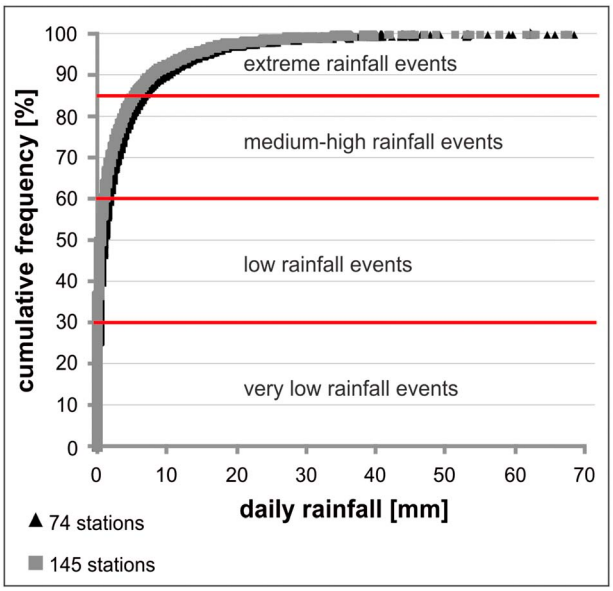

Figure 4. Cumulative distribution of the area average rainfall for 1980–2010 as calculated with the Thiessen Polygons from the 74 and 145 stations.

Following the approach of *Hofstra et al*. [2008], a group of skill scores was selected to evaluate the interpolation techniques. Of the seven scores used in the cited study to evaluate precipitation interpolation, three are also used here: the compound relative error (CRE), the Pearson correlation coefficient (*R*), and the mean absolute error (MAE). A fourth score calculating the mean areal error (MArE) between the modeled and the observed area average rainfall was added. The scores were selected to take into consideration errors both at stations and over the entire area, as well as the goodness of fit between observed and modeled values. A simple and easy readable evaluation system was desired; therefore, the use of different scores targeting approximately the same ability of an interpolation technique (e.g., mean absolute error and root mean square error) was avoided. More indexes could have been considered [e.g., *Hofstra et al*., 2008] but this would have led only to a redundancy in information. In general, the set of scores was constructed following the indications of *Legates and McCabe* [1999], who suggest evaluating models using at least one score for the goodness of fit, one for the absolute error and extra indices furnishing further information on the differences between observations and modeled values (especially in terms of mean and standard deviation). Scores aiming to evaluate methods in terms of capacity to reproduce a wet/dry state or extreme events were not used, because this ability can be considered implicit in the analysis of the four different subsets.

Scores were calculated for each day and then an average daily value was calculated for each score (CRE, *R*, MAE, MArE) for methods ranking purposes. An average rank is finally computed for each technique as the arithmetic mean of the four ranks. Calculating scores for single days avoids problems related to nonstationarity of rainfall events in time. In the presented equations, O are the observed values ($\hat{O}$ the mean), M the modeled values, A the area, n the total number of stations (74 or 145), and i the index for the station. A brief description of the scores is given below.

Compound relative error (CRE): it is a measure of similarity consisting of the ratio between the mean squared error and the variance of the observed data. It is an efficiency measure where the best case is represented by the value of zero, while there is no maximum. Being a measure of fit, it indicates the capacity of a certain technique to reproduce the spatial distribution of the rainfall events, which is particularly important for extreme events — because it determines the areas that might be affected the most — and for local water management. Over a single day, data variability between stations is usually low. This low variability often results in quite high CRE values.

$$\mathrm{CRE} = \frac{\sum_{i=1}^{n} (O_i - M_i)^2}{\sum_{i=1}^{n} \left(O_i - \hat{O}\right)^2} \tag{2}$$

Pearson correlation coefficient (*R*): it measures the correlation between modeled and observed values. It could be considered a measure of potential skill [*Wilks*, 2006] and linear dependence between the two variables, with the best value equal to 1 and the worst value equal to 0. Similar to the CRE, this score evaluates the spatial fit of the model.

$$R = \frac{\sum_{i=1}^{n} O_i M_i - \frac{1}{n}\left(\sum_{i=1}^{n} O_i\right)\left(\sum_{i=1}^{n} M_i\right)}{\left[\sum_{i=1}^{n} O_i^2 - \frac{1}{n}\left(\sum_{i=1}^{n} O_i\right)^2\right]^{0.5}\left[\sum_{i=1}^{n} M_i^2 - \frac{1}{n}\left(\sum_{i=1}^{n} M_i\right)^2\right]^{0.5}} \quad (3)$$

Mean Absolute Error (MAE): it is a measure of average error between modeled and observed values with the best value equal to 0 and without a maximum. It is expressed in the same unit as the analyzed variable. The average daily MAE indicates systematic errors, which can affect the use of the data set for climate applications, while the MAEs of single days can show outliers usually associated with extreme events. This score is therefore useful to differentiate the type of error.

$$\mathrm{MAE} = \frac{1}{n}\sum_{i=1}^{n} |O_i - M_i| \quad (4)$$

Mean Areal Error (MArE): with this score the intention is to measure the effect of each interpolation technique on the water balance, at least from the point of view of inputs, over the entire area of interest. The average area rainfall for each day is calculated with Thiessen's Polygons. This error maintains the same unit of the input precipitation and it is not even an absolute value, allowing also understanding if the methods tend to overestimate (positive values) or underestimate (negative values) the quantity of rainfall affecting the study area. This score is therefore important when evaluating the capacity of the final gridded data set with respect to water resources applications.

$$\mathrm{MArE} = \frac{1}{n} \cdot \frac{\sum_{i=1}^{n} (M_i - O_i) \cdot A_i}{\sum_{i=1}^{n} A_i} \quad (5)$$

To evaluate how the different techniques perform not only in reproducing days with different amounts of rainfall but also how they can be affected by the stations geographical location, two scores were calculated for the set of representative days at each station, individually. The combination of this evaluation with that over days reduces the effect of errors related to spatially inhomogeneous precipitation fields. Specifically, the Critical Compound Error (CRE) and the Normalized Root Mean Squared Error (NRMSE) were selected. In this case, the CRE score indicates how well the different events are reproduced in a certain location. The CRE is computed with equation (2), with the index *i* representing the days and *n* the total number of days (36). For the set of representative days at a single station, the variability of data is quite high, ranging from zero to extreme values. This wide range results in lower CRE scores than those calculated for single days.

Normalized Root Mean Squared Error (NRMSE): it is the well-known Root Mean Squared Error normalized on the range of the observed input values. It is a measure of average error with the best value equal to 0, and the worst equal to 1. It permits an easier comparison of models with different observed input, thus allowing a clear and quick comparison of the different time series registered in different locations. For this reason, it was preferred to MAE, but the information given is almost the same.

$$\mathrm{NRMSE} = \frac{\sqrt{\frac{1}{n}\sum_{i=1}^{n} (O_i - M_i)^2}}{O_{MAX\,i} - O_{MIN\,i}} \quad (6)$$

4. Results and Discussion

4.1. Homogeneity Analysis

The homogeneity analysis did not identify significant breaks in the monthly data that had also a corresponding break in the daily series. However, seven stations had a significant break in their monthly time series and 20 stations a significant break in their daily time series. The metadata of these stations were checked to see if

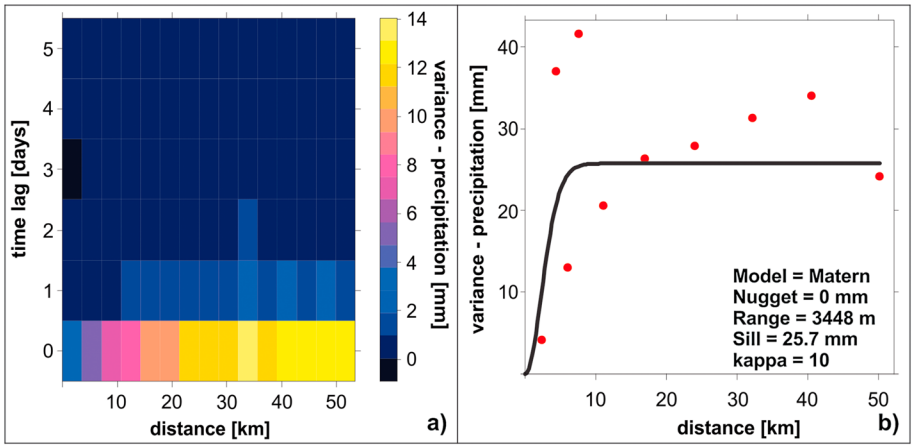

Figure 5. (a) Empirical spatial-temporal variogram calculated for the daily rainfall data of the period 1980–2010; (b) empirical variogram (dots) and automatic fitted variogram model (line) for one of the selected 36 representative days. Model indicates the function used to fit this variogram, while range, sill, and kappa are the parameters requested by the function.

these breaks could be related to a recorded event (e.g., moving of the station, substitution of a manual rain gauge with an automatic one). No correspondence was found between breaks and metadata and so all the stations were maintained. Apparently, the software used for the homogeneity test is quite sensitive to extreme values, as often breaks were recognized in days or months that experienced intense rainfalls.

4.2. Kriging

Ordinary kriging was tested but no satisfactory results were obtained with it. Basically, it was impossible to fit a general spatial-temporal variogram applicable to all days. As it is shown in Figure 5a, data seem to have a very low temporal correlation, which appears even more evident when compared with that calculated for distance. This evidence suggests a fitting of a variogram model for every day. The automap library of R [*Hiemstra*, 2013], which allows an automatic fitting of the variogram, was tested on the 36 representative days. Generally, it worked fine but there were some days with complicated correlation patterns in which a suitable variogram model could not be found (Figure 5b). Therefore, kriging does not seem an appropriate technique to interpolate daily rainfall data in Cyprus. Considering that a number of studies suggest a superiority of some type of kriging (usually ordinary or regression) over other techniques for the interpolation of daily precipitation data [*Rubel et al.*, 2004; *Carrera-Hernandez and Gaskin*, 2007; *Haylock et al.*, 2008; *Symeonakis et al.*, 2009; *Herrera et al.*, 2012], this result is somewhat unexpected. On the other hand, other authors [e.g., *Daly et al.*, 1994; *Shen et al.*, 2001] have also pointed out that smooth interpolation methods are problematic for gridding daily climatic data, due to their high variability in space and time. The range of the variogram in Figure 5b — shorter than 5 km — is an evidence of a strong local component in daily precipitation, which is poorly captured by these techniques. To overcome this problem, *Shen et al.* [2001] proposed a two-step hybrid method, consisting of the interpolation of monthly data by kriging, followed by the temporal downscaling to a daily data set with the use of a proportional regression based on the nearest station assignment method. A possible explanation of the failure of kriging is the nature of rainfall events in Cyprus, which are often limited in space and in time. Events with more than three consecutive rain days are scarce and events are often spatially scattered.

4.3. Evaluation by Days

A comparison between the results obtained performing the interpolation on the complete set of 36 representative days with both the 74 and 145 stations is presented in Table 2 and Figure 6. In the table, for each interpolation method, the values of the calculated scores, with their corresponding rank (#), are presented, as well as their average rank (Ave #). The average area rainfall of the 74 stations for the 36 representative days is 5.13 mm, while the observed average area values for the four subsets are 0.11, 0.71, 3.56, and 24.61 mm. For the 145 stations the area average rainfall of the 36 days is 5.00 mm, while for the four subsets the values are 0.10, 0.67, 3.53, and 23.93 mm.

First, it is clear that the CRE, *R*, and MAE values calculated with 145 stations are considerably better than those obtained with 74 stations. However, this result does not surprise because with more observations a more

Table 2. Summary of the Performance Evaluation of the 14 Methods (See Table 1) for the Modeling of the 36 Representative Days, for 74 and 145 Stations, in Order of Their Average Rank (Ave #)[a]

36 days, 74 stations										36 days, 145 stations									
Method	Ave #	CRE	#	*R*	#	MAE	#	MArE	#	Method	Ave #	CRE	#	*R*	#	MAE	#	MArE	#
		[−]		[−]		[mm]		[mm]				[−]		[−]		[mm]		[mm]	
SWGWR-IDW	**4.3**	0.73	**4**	0.49	**2**	1.73	**3**	0.03	**8**	SWGWR-IDW	**3.5**	0.58	**4**	0.61	**3**	1.29	**2**	0.03	**5**
SWLMR-IDW	**5.3**	0.70	**1**	0.49	**1**	1.80	**9**	0.05	**10**	GWR-IDW	**4.0**	0.62	**6**	0.60	**5**	1.32	**4**	0.01	**1**
TPS	**5.3**	0.76	**7**	0.45	**6**	1.69	**1**	0.02	**7**	IDW	**4.5**	0.57	**1**	0.62	**1**	1.31	**3**	0.15	**14**
SWGWR	**5.5**	0.75	**6**	0.41	**12**	1.73	**2**	−0.01	**2**	SWLMR-IDW	**4.5**	0.57	**2**	0.62	**2**	1.34	**5**	0.06	**10**
GWR-IDW	**6.3**	0.75	**5**	0.49	**4**	1.78	**7**	0.03	**9**	SWGWR-TPS	**5.5**	0.63	**7**	0.58	**6**	0.87	**1**	0.06	**9**
GWR-TPS	**7.3**	0.81	**12**	0.44	**8**	1.79	**8**	0.00	**1**	LMR-IDW	**6.0**	0.58	**3**	0.61	**4**	1.35	**6**	0.06	**11**
LMR-IDW	**7.5**	0.72	**3**	0.48	**5**	1.82	**11**	0.05	**11**	TPS	**6.0**	0.64	**8**	0.57	**7**	1.36	**7**	−0.01	**2**
IDW	**7.8**	0.71	**2**	0.49	**3**	1.85	**12**	0.38	**14**	SWGWR	**7.3**	0.61	**5**	0.53	**12**	1.36	**8**	0.02	**4**
SWGWR-TPS	**7.8**	0.81	**13**	0.43	**9**	1.76	**5**	−0.01	**4**	SWLMR-TPS	**8.5**	0.65	**9**	0.56	**8**	1.41	**11**	0.03	**6**
SWLMR-TPS	**7.8**	0.77	**8**	0.44	**7**	1.74	**4**	0.07	**12**	GWR	**8.8**	0.65	**11**	0.54	**11**	1.40	**10**	0.02	**3**
GWR	**8.3**	0.78	**9**	0.43	**11**	1.81	**10**	0.01	**3**	GWR-TPS	**9.5**	0.67	**12**	0.56	**10**	1.39	**9**	0.03	**7**
LMR-TPS	**10.0**	0.79	**11**	0.43	**10**	1.77	**6**	0.08	**13**	LMR-TPS	**9.8**	0.65	**10**	0.56	**9**	1.41	**12**	0.04	**8**
SWLMR	**10.8**	0.78	**10**	0.36	**14**	2.02	**13**	−0.02	**6**	SWLMR	**13.0**	0.74	**13**	0.41	**14**	1.84	**13**	0.08	**12**
LMR	**11.5**	0.81	**14**	0.36	**13**	2.07	**14**	−0.02	**5**	LMR	**13.5**	0.75	**14**	0.42	**13**	1.86	**14**	0.08	**13**

[a]# represents the rank, CRE the critical compound error, R the Pearson's correlation coefficient, MAE the mean absolute error, and MArE the mean areal error. Ranks are in bold to increase the readability of the table.

precise estimate is expected. Figure 6 also shows, for each technique, a reduction in the variability of the scores (it is particularly evident for *R*) with a higher number of stations. This is due to a more regular and dense coverage of the study area, which allows a more homogeneous interpolation of events characterized by different amounts of rainfall and spatial distribution. The lower variance shown by the scores using 145 stations helps to identify good methods such as IDW, SWGWR-IDW, and SWLMR-IDW. Similarly, for the MArE score, the additional information available with a higher number of stations results in smaller outliers (Figure 6).

For the 36 representative days together, the best method is the SWGWR-IDW, for both station densities (Table 2). Other similarities between the two station densities are the poor performance of the linear multiple regression method, with or without the application of the stepwise procedure, both alone and when coupled with TPS. Geographically weighted regression usually performs better. This is coherent with findings of other authors treating the interpolation of precipitation and other climate variables, even if with a different temporal resolution [*Bostan et al.*, 2012; *Szymanowski and Kryza*, 2012]. Conversely, the main differences are that TPS performs very well with 74 stations (second best method with the same average rank as SWLMR-IDW), while it is ranked sixth with the 145 stations. The opposite behavior is shown by IDW, performing well with 145 stations but not as well with 74.

Regarding IDW, an increase in stations density reduces the search radius, at least when performing an estimate with a fixed number of observations (12). In fact, by almost doubling the stations number, the observations used for estimation are much closer in space to the point needing the estimate. In this sense, the result obtained is describing a very strong local component in Cyprus precipitation. On the other hand, TPS gives the impression to result in a general smooth precipitation surface, therefore performing relatively better with more separated stations and more spatially continuous precipitation fields (high rainfall events). The smoothing effect of TPS is above all revealed by the good rank positions obtained for the MArE score, where positive and negative errors balance each other (Tables 2 and 3). The general tendency of TPS to oversmooth the created surface with respect to the observations was already pointed out by other authors [e.g., *Perry and Hollis*, 2005].

Table 3 shows the results obtained using the four subsets for 145 stations. The ranking of the different techniques appears quite stable moving through the subsets. The best method for the very low, low, and medium-high rainfall events is always simple IDW. Moreover, in the best five methods (with only two exceptions), the same techniques (IDW, SWGWR-IDW, SWLMR-IDW, GWR-IDW, and SWGWR) are always present. Major differences can be noticed only when reproducing high rainfall events (area average rainfall ranging from ~5 to ~70 mm). For this case, the IDW technique does not perform as well and the SWGWR-IDW method becomes the best method, similar as for the full set of 36 days (Table 2). This result demonstrates the relatively high importance of the few events characterized by high rainfall amounts when evaluating all days together.

The MArE score in Table 3 indicates that the interpolation techniques tend to overestimate low and medium rainfall events and underestimate high rainfall events. However, the behavior of the fit scores (CRE and *R*) in

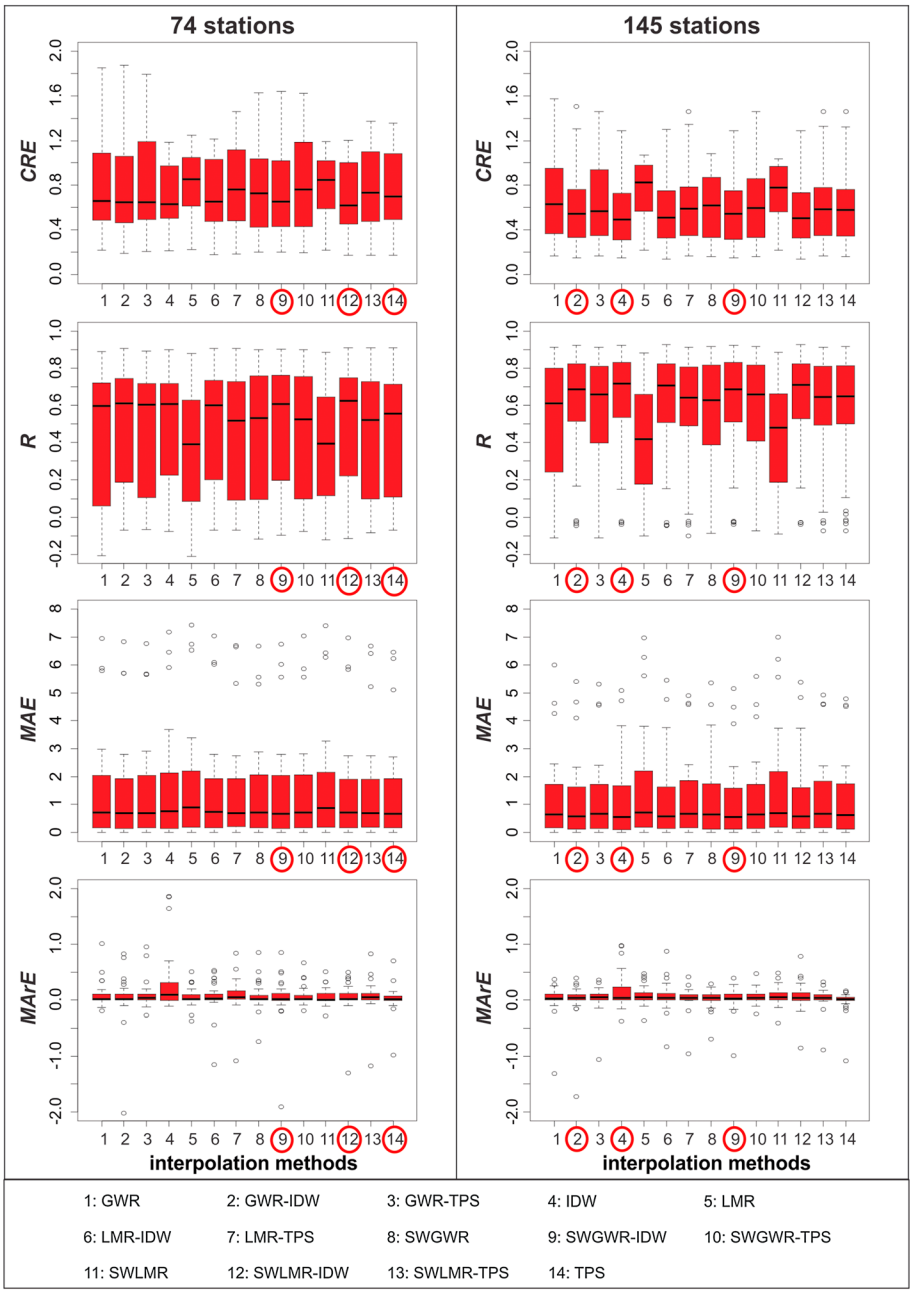

Figure 6. Modified boxplots showing the distribution of the scores calculated, over the 36 representative days, with the different interpolation techniques, for (left panel) 74 and (right panel) 145 stations. The boxes represent the interquartile range (IQR), whiskers extend 1.5 · IQRs, while the circles are the outliers. For the meaning of the acronyms of the techniques, refer to Table 1. The circled techniques on the *x* axis are the best three in terms of average rank (see Table 2).

the different subsets is giving different indications. It is evident that the quality of fit increases with increasing area average rainfall. This testifies that all techniques have more problems in capturing the spatial distribution of rainfall events that are not widespread over the area of interest, but localized in specific areas. When considering these spotted rainfalls, the results obtained testify that with a sufficient density of stations these events can be reproduced well by simple IDW.

The scores shown for IDW and SWGWR-IDW in Table 3 indicate that splitting the interpolation performing IDW for very low to medium rainfall events and SWGWR-IDW for high events results in the best possible reproduction of the spatial distribution of rainfall (top rank for both CRE and *R* in any subset). A well-covered

Table 3. Summary of the Performances Evaluation of the 14 Methods (See Table 1) for the Four Subsets of Representative Days[a]

Very Low Rainfall Events — 0–30%

Method	Ave #	CRE	#	R	#	MAE	#	MArE	#
		[−]		[−]		[mm]		[mm]	
IDW	**1.5**	0.81	**1**	0.41	**1**	0.08	**1**	0.02	**3**
SWGWR-IDW	**2.3**	0.81	**2**	0.41	**3**	0.08	**2**	0.01	**2**
SWLMR-IDW	**4.8**	0.81	**3**	0.41	**2**	0.09	**5**	0.02	**9**
SWGWR	**5.5**	0.85	**5**	0.20	**12**	0.09	**4**	0.01	**1**
SWGWR-TPS	**6.0**	0.90	**6**	0.34	**6**	0.09	**7**	0.02	**5**
GWR-IDW	**6.3**	0.91	**10**	0.36	**5**	0.09	**3**	0.02	**7**
TPS	**6.3**	0.91	**8**	0.33	**7**	0.09	**6**	0.02	**4**
LMR-IDW	**7.0**	0.82	**4**	0.40	**4**	0.09	**8**	0.03	**12**
GWR	**9.8**	0.98	**13**	0.23	**11**	0.10	**9**	0.02	**6**
SWLMR	**10.5**	0.91	**7**	0.11	**14**	0.11	**13**	0.02	**8**
SWLMR-TPS	**10.8**	0.92	**11**	0.33	**8**	0.10	**11**	0.03	**13**
LMR-TPS	**11.0**	0.91	**9**	0.33	**9**	0.10	**12**	0.03	**14**
GWR-TPS	**11.3**	1.02	**14**	0.28	**10**	0.10	**10**	0.03	**11**
LMR	**12.3**	0.93	**12**	0.18	**13**	0.11	**14**	0.03	**10**

Low Rainfall Events — 31–60%

Method	Ave #	CRE	#	R	#	MAE	#	MArE	#
		[−]		[−]		[mm]		[mm]	
IDW	**2.0**	0.62	**1**	0.59	**1**	0.48	**1**	0.02	**5**
SWGWR-IDW	**4.0**	0.64	**5**	0.58	**5**	0.50	**3**	0.02	**3**
GWR-IDW	**4.0**	0.64	**4**	0.58	**4**	0.49	**2**	0.03	**6**
SWLMR-IDW	**4.3**	0.62	**2**	0.59	**2**	0.52	**4**	0.05	**9**
GWR	**5.5**	0.65	**6**	0.55	**7**	0.52	**7**	0.02	**2**
LMR-IDW	**5.5**	0.63	**3**	0.58	**3**	0.52	**6**	0.05	**10**
TPS	**6.5**	0.71	**10**	0.52	**10**	0.52	**5**	0.00	**1**
GWR-TPS	**7.3**	0.68	**8**	0.55	**6**	0.53	**8**	0.03	**7**
SWGWR	**7.5**	0.67	**7**	0.53	**9**	0.55	**10**	0.02	**4**
SWGWR-TPS	**8.5**	0.69	**9**	0.54	**8**	0.54	**9**	0.03	**8**
LMR-TPS	**11.5**	0.73	**12**	0.52	**12**	0.56	**11**	0.05	**11**
SWLMR-TPS	**12.0**	0.72	**11**	0.52	**11**	0.56	**14**	0.05	**12**
SWLMR	**12.8**	0.80	**13**	0.41	**13**	0.67	**12**	0.06	**13**
LMR	**13.8**	0.81	**14**	0.39	**14**	0.68	**13**	0.06	**14**

Medium-High Rainfall Events — 61–84%

Method	Ave #	CRE	#	R	#	MAE	#	MArE	#
		[−]		[−]		[mm]		[mm]	
IDW	**4.3**	0.39	**1**	0.78	**1**	1.68	**2**	0.20	**13**
SWLMR-IDW	**4.8**	0.39	**2**	0.78	**2**	1.71	**3**	0.20	**12**
SWGWR-IDW	**5.0**	0.41	**4**	0.77	**4**	1.67	**1**	0.17	**11**
SWGWR	**5.3**	0.42	**5**	0.75	**6**	1.73	**6**	0.13	**4**
GWR-IDW	**5.3**	0.42	**7**	0.76	**5**	1.72	**4**	0.14	**5**
LMR-IDW	**6.3**	0.40	**3**	0.78	**3**	1.73	**5**	0.21	**14**
TPS	**6.8**	0.44	**8**	0.74	**9**	1.81	**9**	0.05	**1**
GWR	**7.3**	0.44	**10**	0.74	**10**	1.80	**7**	0.08	**2**
SWGWR-TPS	**7.3**	0.42	**6**	0.75	**7**	1.81	**8**	0.14	**8**
GWR-TPS	**7.5**	0.44	**9**	0.75	**8**	1.89	**10**	0.11	**3**
SWLMR-TPS	**10.0**	0.45	**11**	0.73	**11**	1.89	**11**	0.14	**7**
SWLMR	**11.0**	0.65	**13**	0.57	**13**	2.45	**12**	0.14	**6**
LMR-TPS	**11.5**	0.45	**12**	0.73	**12**	2.46	**13**	0.16	**9**
LMR	**13.0**	0.66	**14**	0.56	**14**	2.48	**14**	0.16	**10**

High Rainfall Events — 85–100

Method	Ave #	CRE	#	R	#	MAE	#	MArE	#
		[−]		[−]		[mm]		[mm]	
SWGWR-IDW	**2.5**	0.27	**1**	0.85	**1**	4.50	**1**	−0.10	**7**
LMR-IDW	**3.0**	0.28	**2**	0.85	**4**	4.73	**5**	−0.03	**1**
SWLMR-IDW	**3.5**	0.29	**3**	0.85	**3**	4.74	**6**	−0.04	**2**
IDW	**5.8**	0.29	**4**	0.85	**2**	4.67	**3**	0.58	**14**
GWR-IDW	**6.0**	0.29	**5**	0.84	**5**	4.66	**2**	−0.19	**12**
SWGWR	**6.8**	0.30	**7**	0.84	**7**	4.77	**7**	−0.09	**6**
TPS	**7.3**	0.30	**6**	0.84	**6**	4.68	**4**	−0.19	**13**
SWLMR-TPS	**8.5**	0.30	**8**	0.84	**8**	4.78	**8**	−0.14	**10**
GWR-TPS	**9.0**	0.32	**11**	0.83	**11**	4.84	**10**	−0.05	**4**
SWGWR-TPS	**9.0**	0.30	**10**	0.83	**10**	4.84	**11**	0.06	**5**
LMR-TPS	**9.5**	0.30	**9**	0.83	**9**	4.80	**9**	−0.15	**11**
GWR	**9.8**	0.33	**12**	0.82	**12**	4.93	**12**	−0.05	**3**
SWLMR	**11.8**	0.43	**13**	0.75	**13**	6.45	**13**	0.12	**8**
LMR	**12.8**	0.43	**14**	0.75	**14**	6.49	**14**	0.12	**9**

[a]The results obtained with 145 stations are shown here; # represents the rank, CRE the critical compound error, *R* the Pearson's correlation coefficient, MAE the mean absolute error, and MArE the mean areal error. Ranks are in bold to increase the readability of the table.

areal distribution is particularly important for extreme events and also affects water management applications. Using the two techniques for different events, also the MAE is minimized. A small average MAE calculated over all the days (Table 3), coupled with a narrow interquartile range (IDW — Figure 6) means a small systematic error, which is particularly good for climate applications. On the other hand, Figure 6 shows that the MAE outliers for the SWGWR-IDW are usually lower than those of the other techniques. This means that the method is capable of reproducing peak precipitation well, making the suggested combination of techniques particularly suitable also for the study of processes related to extreme events (flood forecasting, triggering of landslides, etc.). The only score with a nonoptimum ranking is the MArE, which can affect water resources applications. However, except for one subset, the ranking of the selected techniques for this score is in the best half. The proposed combination of methods seems therefore the best possible compromise for all possible applications of the gridded data set.

The good performance of IDW, both alone and combined with a regression technique, is a confirmation of the quality of this simple method for complex topographical areas with sufficient station density. The importance of station density when applying this method was already revealed by *Daly* [2006]. Inverse distance weighting was also selected by *Perry et al.* [2009] to model precipitation on a daily basis over the UK, and its spherical version was used by *Frei and Schär* [1998] to model daily precipitation over the Alps. In both these studies, station density was high.

4.4. Evaluation by Stations

The map of the station CREs (Figure 7) shows that the top four methods perform quite uniformly and homogenously all over the study area, with the exception of few observation points located in the

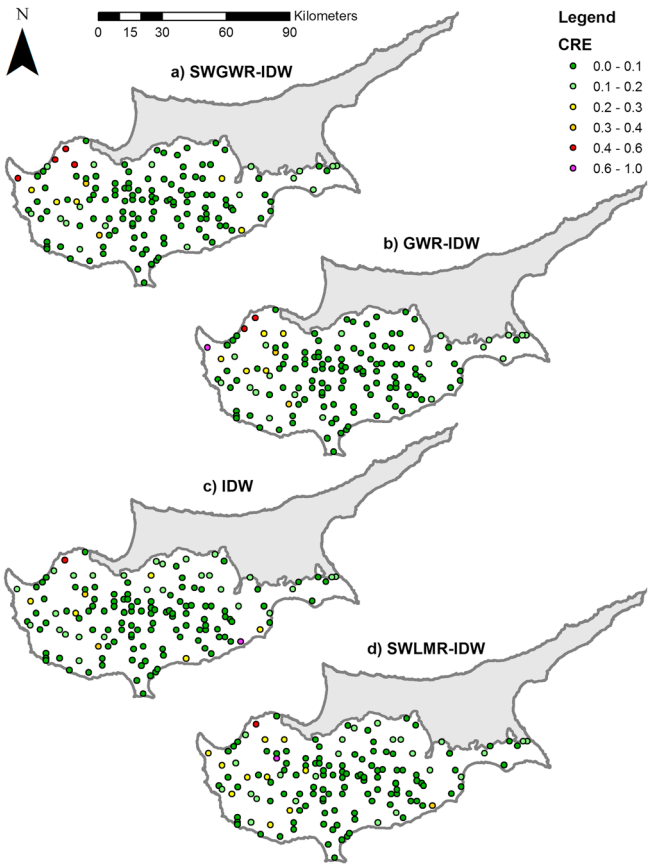

Figure 7. Map showing the calculated compound relative error values at the 145 stations for the best four interpolation methods considering all the 36 representative days. (a) SWGWR-IDW, (b) GWR-IDW, (c) IDW, (d) SWLMR-IDW.

mountainous north-west. This area is characterized by many valleys, quite close to each other and rather deep. Average elevation is also increasing rapidly and the density of stations is low. For these reasons the estimation of a single station can depend on observations that can differ from each other, mainly due to geographical characteristics. In this area, in fact, it is not only CRE that shows quite high values but also NRMSE (Figure 8), underlining that the problem is not only related to possible outliers but is more general. Simple IDW shows also poor CRE and NRMSE values in the central-north part of the country, in the Mesaoria Plain. In this case, the high errors are again mainly due to a low density of the stations but the simpler topography allows the techniques with a regression step to limit the discrepancies between observed and modeled values. Other more local errors, limited to a single or a couple of neighboring stations, are due to high rainfall events not perfectly reproduced by the interpolation techniques. The CRE scores are particularly useful for locating these kinds of errors; CRE is in fact quite sensitive to outliers [*Murphy and Epstein*, 1989; *Schmidli et al*., 2001; *Hofstra et al*., 2008]. Looking at Figures 7 and 8, it is therefore clear that errors are more dependent on the local stations density than on any other characteristics.

4.5. Final Data Set

The evaluation on the 36 representative days and the four subsets indicates that for 145 stations SWGWR-IDW is the best method to interpolate high rainfall events, and simple IDW is the best method for low and medium rainfalls. Our final gridded data set was constructed according to these findings.

These results, obtained from the score evaluation method, deserve a further analysis. In Figure 9, the interpolated six extreme events, obtained using the SWGWR-IDW technique and all 145 stations, are shown. The event of 1 December 1992 is the highest rainfall event recorded for the studied period. Probability density functions of the gauges in the highest rainfall areas indicate return periods around 40 years for the observed amounts [*Pashiardis*, 2009]. The selected parameters of the regression equations are presented as well. Four

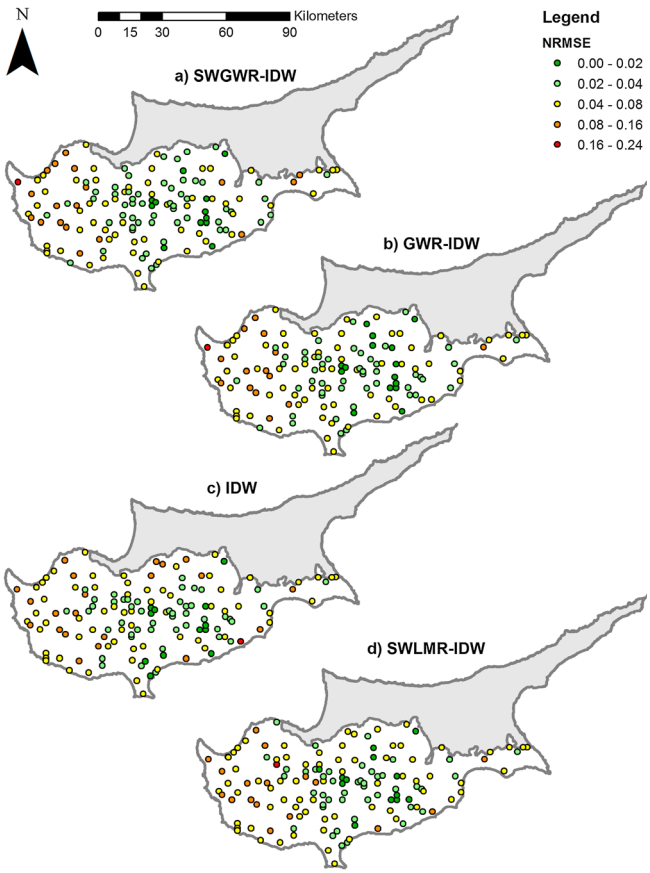

Figure 8. Map showing the calculated NRMSE values at the 145 stations for the best four interpolation methods considering all the 36 representative days. (a) SWGWR-IDW, (b) GWR-IDW, (c) IDW, and (d) SWLMR-IDW.

out of six high events show exactly the same parameter set with 74 and 145 stations, while the other two differ only for an extra variable present when using 145 stations (the underlined variable in Figure 9). Elevation is the main influencing variable, being always present and indicating a permanent orographic effect in this type of events. Also, a variable indicating the presence of a general spatial pattern, probably revealing the direction of movement of the humid fronts, is always present. In fact, both the north and the east coordinate variables are present in five out of six analyzed days (in four cases together). Other processes, such as the land-sea effect or the mountain-shadow effect, are less regular and their influence seems to vary from event to event.

Although simple IDW was used to interpolate very low, low, and medium-high rainfalls, it is interesting to quickly analyze the step-wise equations calculated for these days to further strengthen this choice. The equations can be very different using the two sets of observations (74 and 145 stations). In six extreme cases (three for very low events, two for low events, and one for a medium-high event), the two equations for the same day have absolutely no variables in common. There is therefore a clear distinction between large-scale events, which undoubtedly depend on synoptic processes that can be captured by a certain set of geographical variables, and local events that are poorly related to geographical factors.

As a further evaluation of the final data set, the relative error of precipitation frequency [*Rupp et al*., 2010] was calculated. This error is defined as the ratio of the difference between the numbers of observed and modeled rainfall days and the number of observed days with rainfall. Negative values denote an excess of modeled rainy days. This evaluation was based on the 36 representative days, 145 stations, and cross validation. The threshold to consider a day as a wet day was put at 0.2 mm, consistent with the readability of the used rain gauges. For the combination of proposed methods (SWGWR-IDW for high events, IDW for all others), the obtained mean relative error is −0.14, indicating a slight overestimation of the wet days at certain locations.

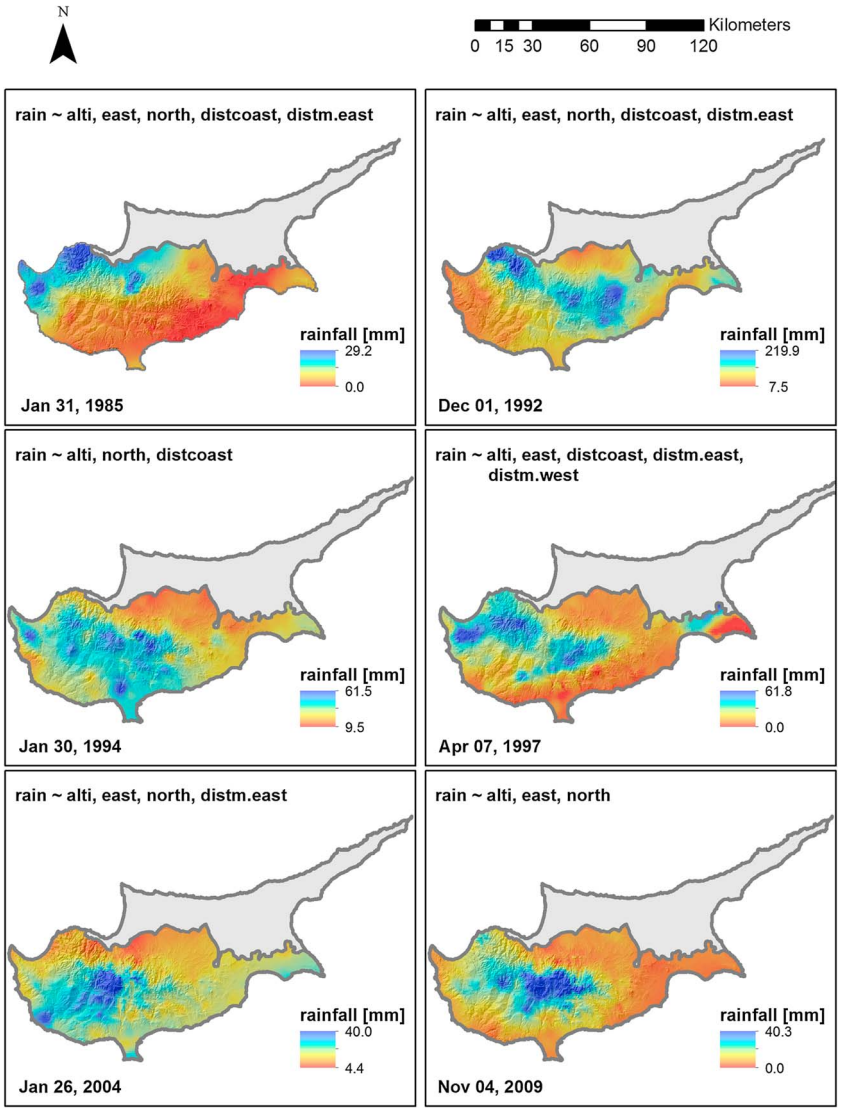

Figure 9. The six high rainfall events present in the subset of representative days interpolated through SWGWR-IDW. The variables of the step-wise regression equation used for each event are shown as well. The underlined variables are present only for the 145 stations analysis. Alti is the elevation; east and north are the east and north coordinates, respectively; distcoast is the distance from the coast; and distm.east and distm.west are the distances from the main ridge of the mountain chain to the east and to the west, respectively.

The error is decreasing, in absolute terms, with increasing rainfall; excluding the high events it becomes −0.22. The results show that most of the false alarms (recognizing a wet day on a dry day) occur during low rainfall events. The erroneous rain averaged 0.77 mm per day over all stations, (with a minimum and maximum at a single site of 0.11 and 4.75 mm, respectively). This is much lower than the daily evapotranspiration rate and will have little effect on the quality of the created gridded data set for agricultural and water resources applications.

Concluding, even if SWGWR-IDW is the overall best performing method (Table 2) and it does not score so differently from IDW for low and medium rainfall events (Table 3), the stability of IDW when modeling days with little rainfall, and the physical implications in adopting a combined regression-neighboring interpolation method favored the choice of interpolating local and large-scale events with different techniques.

In Figure 10, two maps extracted from the complete database are presented. In Figure 10a, a low rainfall day modeled with IDW, while in Figure 10b, an extreme event modeled with SWGWR-IDW. The two events are very different. The low rainfall is a typical Spring-Summer event with a maximum on the mountains and a relatively higher abundance of rainfall on the eastern side of the mountains than on the western flank. In the

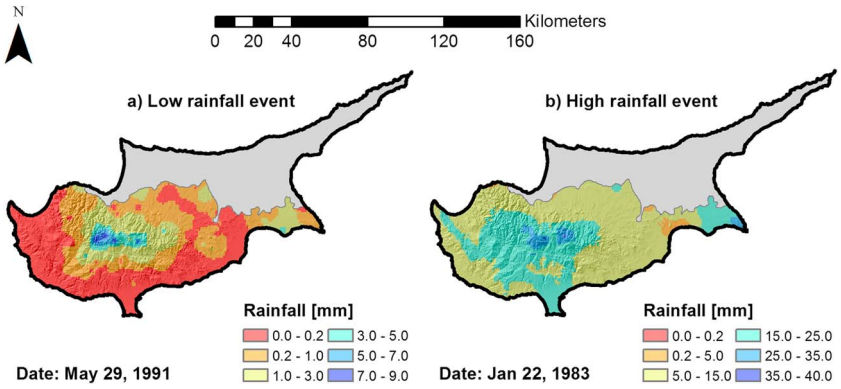

Figure 10. (a) A low rainfall event modeled with IDW (48th percentile) and (b) an extreme rainfall event modeled with SWGWR-IDW (95th percentile). The lowest class is considered the no-rainfall class; the limit of 0.2 mm was selected because of the rainfall gauges readability.

Mesaoria Plain, rainfall does not behave as a perfectly continuous field and some no-rainfall cells occur in the middle of rainy areas. Inverse Distance Weighting is very dependent on the observation values and this creates the already cited problems in reconstructing the spatial pattern of spotted rainfalls. Nevertheless, the difference in the rainfall amount is so small that this behavior of rainfall if not probable can be considered at least possible. The high event (Figure 10b) is a typical winter occurrence arriving as a humid front from the south-west, with the maximum rainfall on the top of the mountains. Mountains play a barrier effect but rainfall is widespread all over the country with lower values. In this case, sparse points with different rainfall amounts are less evident. This is another proof that widespread rainfall events are better reproduced by combined interpolation techniques.

5. Conclusions

A comparison of different interpolation techniques for the creation of a gridded data set of daily precipitation with a resolution of 1×1 km^2 over Cyprus was presented. The techniques tested and evaluated comprise regression (linear multiple and geographically weighted), and neighboring interpolators (inverse distance weighting, kriging, and 3D thin plate splines). Regressions and neighboring interpolators were used both individually and combined. Techniques were evaluated using two different stations densities (0.0125 and 0.0246 station/km^2) over 36 representative days, selected based on percentiles of area-average rainfall.

In general, the two main sources of error when interpolating daily data seem related to very local, difficult-to-predict changes in rainfall amount, and to areas with low station densities. In this regard, the comprehensive cross-validation approach (by days and by stations) applied in this study can also contribute to the optimization of the rain gauge network.

A change in the number of rainfall stations modified the relative ranking of the methods, allowing to state that the best performing interpolation technique can be considered a function not only of the topographical complexity of an area and the target spatial scale, as reported by *Vicente-Serrano et al*. [2003], but also of the observations density available for the interpolation. Increasing the number of stations used for interpolation led also to a greater stability in the rank of the various techniques, when considering events characterized by different rainfall amounts. This stability in the ranking was lost only when analyzing high rainfall events. The reason is mainly related to the different spatial patterns of high and low rainfall events, as high events are usually characterized by a more uniform coverage of rainfall over the study area.

For both station densities, all interpolation methods performed better with increasing average rainfall over the area of interest. The error between observed and modeled values in absolute terms increases, but the quality of fit due to the capability of reproducing the observed spatial pattern of precipitation improves. This is mainly due to the characteristics of the precipitation events that pass from being more localized to being more widespread. Very local and scattered events are difficult to be reproduced by any method, whether the analyzed event is small or large. This is also because these small events are difficult to relate to geographical variables that could describe the processes leading to precipitation.

This study clearly shows how results can be affected by considering different rainfall events, characterized by different rainfall amounts, different spatial variability, and different densities in the original observation data. This study allows to point out the importance of differentiating between high rainfall events, characterized by high cumulated daily rainfall and covering a large areas, and more local events with lower cumulated (over the whole area) rainfall. The high rainfall events are mainly frontal events, while the others can be generically classified as convective events. The two types of events are best interpolated with different methods and it is crucial to use, in each situation, the best performing technique. The high events are few but they bring a lot of water with them, so small relative errors can cause quite high errors in terms of water input. On the other hand, the low and medium events are much more frequent and even if they bring less water than the high events, the sum of consecutive errors can heavily affect the total water input. The best method for interpolating high, spatially distributed events was SWGWR-IDW, while for the other events a simple IDW interpolation was adopted. Physical variables can describe spatially distributed events very well, but their influence is not clearly recognizable when interpolating local events.

The scores used for the evaluation of the interpolation techniques target different possible applications of the final gridded data set, including water resources management, agricultural planning, climate analyses, and flood management. The proposed combination of methods is the optimum solution for all applications except those related to water resources, for which, in any case, it remains a very good compromise, considering that the calculated daily error is much lower than the daily evapotranspiration rate.

Cyprus is a very good site for deriving general guidelines to assist with the selection of interpolation methods for daily precipitation in other locations. In this sense, this work presents a wide range of possible combinations of rainfall regimes, topographical and geographical characteristics, and available observations that can be transferred to applications in different areas around the world. According to the results obtained, general indications for the selection of an interpolation technique for rainfall data can be summarized as follows:

1. Station density and rainfall amount are the two main factors for the selection of a spatial interpolation method;
2. It is important to analyze possible differences in the performance of interpolation methods for low (local) and high (large-scale) rainfall events;
3. Simple topography and low station density (~0.015 station/km^2) are expected to favor smoothing techniques;
4. A careful evaluation of the fitting of variogram models is strongly suggested before using KR;
5. GWR is likely to perform better than LMR, especially in topographical complex areas due to its nonstationarity in space;
6. A step-wise selection of regression variables usually provides robust parsimonious models and reduces overfitting;
7. A certain interpolation technique can represent high rainfalls well and low events poorly, or vice versa;
8. Local (convective) events are difficult to link to geographical variables;
9. Given a relatively high station density (~0.025 station/km^2), local (convective) events are usually well reproduced by simple IDW.
10. The use of a step-wise regression model, based on physical variables, can help the interpolation of large-scale events;
11. Large-scale events are usually influenced by elevation and a general spatial pattern, well described by geographical coordinates; factors such as land-sea and mountain shadow effects play a less frequent role.

The gridded (1×1 km^2) data set provides a climatological reference for climate change impact and adaptation studies. The selected interpolation methods will also be used to create data sets for future periods using global climate model results dynamically downscaled through Regional Climate Models (RCMs).

Acknowledgments

This work is part of the AGWATER project (ΑΕΙΦΟΡΙΑ/ΓΕΩΡΓΟ/0311(BIE)/06), cofinanced by the European Regional Development Fund and the Republic of Cyprus through the Research Promotion Foundation. The authors would like to thank Evangelios Tyrlis and Andries De Vries for their time and support in the discussion and presentation of Cyprus climatology. We would also like to express our appreciation to Silas Michaelides and the staff of the Cyprus Meteorological Service for the management of the observational network. Gratitude is also extended to the editor and the three anonymous reviewers who helped to improve the quality of the manuscript.

References

Agnew, M. D., and J. P. Palutikof (2000), GIS-based construction of baseline climatologies for the Mediterranean using terrain variables, *Clim. Res.*, *14*, 115–127, doi:10.3354/cr014115.

Akaike, H. (1970), Statistical predictor identification, *Ann. Inst. Stat. Math.*, *22*, 203–217, doi:10.1007/BF02506337.

Avellan, T., F. Zabel, and W. Mauser (2012), The influence of input data quality in determining areas suitable for crop growth at the global scale – A comparative analysis of two soil and climate datasets, *Soil Use Manage.*, *28*, 249–265, doi:10.1111/j.1475-2743.2012.00400.x.

Barnett, T., et al. (2005), Detecting and attributing external influences on the climate system: A review of recent advances, *J. Clim.*, *18*, 1291–1314.

Bivand, R., and D. Yu (2013), SpGWR: Geographically weighted regression. R package version 0.6-20. [Available at http://cran.r-project.org/web/packages/spgwr/spgwr.pdf.]
Bostan, P. A., G. B. M. Heuvelink, and S. Z. Akyurek (2012), Comparison of regression and kriging techniques for mapping the average annual precipitation of Turkey, *Int. J. Appl. Earth Obs. Geoinf.*, *19*, 115–126, doi:10.1016/j.jag.2012.04.010.
Brown, D. P., and A. C. Comrie (2002), Spatial modelling of winter temperature and precipitation in Arizona and New Mexico, USA, *Clim. Res.*, *22*, 115–128, doi:10.3354/cr022115.
Bruggeman, A., C. Zoumides, S. Pashiardis, P. Hadjinicolaou, M. A. Lange, and T. Zachariadis (2011), Effect of climate variability and climate change on crop production and water resources in Cyprus, Study commissioned by the Ministry of Agriculture, Natural Resources and Environment of Cyprus, led by the Agricultural Research Institute, Nicosia, Cyprus. [Available at: http://eewrc.cyi.ac.cy/system/files/Bruggeman_etal_climate_and_agriculture_Cyprus_Jun2011.pdf.]
Brunsdon, C., A. S. Fotheringham, and M. Charlton (1996), Geographically weighted regression: A method for exploring spatial non-stationarity, *Geog. Anal.*, *28*, 281–298.
Bussières, N., and W. Hogg (1989), The objective analysis of daily rainfall by distance weighting schemes on a mesoscale grid, *Atmos. Ocean*, *27*, 521–541.
Carrera-Hernandez, J. J., and S. J. Gaskin (2007), Spatio temporal analysis of daily precipitation and temperature in the Basin of Mexico, *J. Hydrol.*, *336*, 231–249, doi:10.1016/j.jhydrol.2006.12.021.
Charlton, M., and A. S. Fotheringham (2009), *Geographically Weighted Regression White Paper*, Science Foundation Ireland, Ireland, (http://ncg.nuim.ie/ncg/GWR/GWR_WhitePaper.pdf).
Daly, C. (2006), Guidelines for assessing the suitability of spatial climate data sets, *Int. J. Climatol.*, *26*, 707–721, doi:10.1002/joc.1322.
Daly, C., R. P. Neilson, and D. L. Phillips (1994), A statistical-topographic model for mapping climatological prediction over mountainous terrain, *J. Appl. Meteorol.*, *33*, 140–158, doi:10.1175/1520-0450(1994)033<0140:ASTMFM>2.0.CO;2.
Fader, M., S. Rost, C. Müller, A. Bondeau, and D. Gerten (2010), Virtual water content of temperate cereals and maize: Present and potential future patterns, *J. Hydrol.*, *384*, 218–231, doi:10.1016/j.jhydro1.2009.12.011.
Fotheringham, A. S., C. Brunsdon, and M. Charlton (2002), *Geographically Weighted Regression: The Analysis of Spatially Varying Relationships*, Wiley, Chichester.
Frei, C., and C. Schär (1998), A precipitation climatology of the alps from high-resolution rain-gauge observations, *Int. J. Climatol.*, *18*, 873–900, doi:10.1002/(SICI)1097-0088(19980630)18:8<873::AID-JOC255>3.0.CO;2–9.
Fundel, F., A. Walser, M. A. Liniger, C. Frei, and C. Appenzeller (2010), Calibrated precipitation forecasts for a limited-area ensemble forecast system using reforecasts, *Mon. Weather Rev.*, *138*, 176–189, doi:10.1175/2009MWR2977.1.
Goovaerts, P. (2000), Geostatistical approaches for incorporating elevation into the spatial interpolation of rainfal, *J. Hydrol.*, *228*, 113–129, doi:10.1016/S0022-1694(00)00144-X.
Gosling, S. N., and N. W. Arnell (2011), Simulating current global river runoff with a global hydrological model: model revisions, validation, and sensitivity analysis, *Hydrol. Processes*, *25*, 1129–1145, doi:10.1002/hyp.7727.
Gritti, E. S., B. Smith, and M. T. Sykes (2006), Vulnerability of Mediterranean Basin ecosystems to climate change and invasion by exotic plant species, *J. Biogeogr.*, *33*, 145–157, doi:10.1111/j.1365-2699.2005.01377.x.
Hadjinicolaou, P., C. Giannakopoulos, C. Zerefos, M. A. Lange, S. Pashiardis, and J. Lelieveld (2011), Mid-21st century climate and weather extremes in Cyprus as projected by six regional climate models, *Reg. Environ. Change*, *11*, 441–457, doi:10.1007/s10113-010-0153-1.
Harris, P., A. S. Fotheringham, R. Crespo, and M. Charlton (2010), The use of geographically weighted regression for spatial prediction: An evaluation of models using simulated data sets, *Math. Geosci.*, *42*, 657–680, doi:10.1007/s11004-010-9284-7.
Haylock, M. R., N. Hofstra, A. M. G. Klein Tank, E. J. Klok, P. D. Jones, and M. New (2008), A European high resolution gridded data set of surface temperature and precipitation for 1950–2006, *J. Geophys. Res.*, *113*, D20119, doi:10.1029/2008JD010201.
Herrera, S., J. M. Gutiérrez, R. Ancell, M. R. Pons, M. D. Frías, and J. Fernández (2012), Development and analysis of a 50-year high-resolution daily gridded precipitation dataset over Spain (Spain02), *Int. J. Climatol.*, *32*, 74–85, doi:10.1002/joc.2256.
Hiemstra, P. (2013), Automap: Automatic interpolation package. R package version 1.0-12. [Available at http://cran.r-project.org/web/packages/automap/automap.pdf.]
Hofstra, N., M. Haylock, M. New, P. Jones, and C. Frei (2008), Comparison of six methods for the interpolation of daily European climate data, *J. Geophys. Res.*, *113*, D21110, doi:10.1029/2008JD010100.
Hurvich, C. M., J. S. Simonoff, and C. L. Tsai (1998), Smoothing parameter selection in nonparametric regression using an improved Akaike information criterion, *J. R. Stat. Soc. Series B*, *60*, 271–293, doi:10.1111/1467-9868.00125.
Hutchinson, M. F. (1991), The application of thin plate smoothing splines to continent wide data assimilation, in *Data Assimilation Systems, BMRC Research Report No. 27*, edited by J. D. Jasper, pp. 104–113, Bureau of Meteorology, Melbourne.
Hutchinson, M. F. (1993), On thin plate splines and kriging, in *Computing Science and Statistics*, vol. 25, edited by M. E. Tarter and M. D. Lock, pp. 55–62, Berkeley, Interface Foundation of North America, University of California.
Hutchinson, M. F. (1995), Stochastic space-time weather models from ground-based data, *Agr. For. Meteorol.*, *73*, 237–264, doi:10.1016/0168-1923(94)05077-J.
Jarvis, C. H., and N. Stuart (2001), A comparison among strategies for interpolating maximum and minimum daily air temperatures. Part II: The interaction between number of guiding variables and the type of the interpolation method, *J. Appl. Meteorol.*, *40*, 1075–1084, doi:10.1175/1520-0450(2001)040<1075:ACASFI>2.0.CO;2.
Kiktev, D., D. M. H. Sexton, L. Alexander, and C. K. Folland (2003), Comparison of modeled and observed trends in indices of daily climate extremes, *J. Clim.*, *16*, 3560–3571, doi:10.1175/1520-0442(2003)016<3560:COMAOT>2.0.CO;2.
Kilsby, C. G., P. D. Jones, A. Burton, A. C. Ford, H. J. Fowler, C. Harpham, P. James, A. Smith, and R. L. Wilby (2007), A daily weather generator for use in climate change studies, *Environ. Modell. Software*, *22*, 1705–1719, doi:10.1016/j.envsoft.2007.02.005.
Kizza, M., I. Westerberger, A. Rodhe, and H. K. Ntale (2012), Estimating areal rainfall over Lake Victoria and its basin using ground-based and satellite data, *J. Hydrol.*, *464–465*, 401–411, doi:10.1016/j.jhydrol.2012.07.024.
Krige, D. G. (1951), A statistical approach to some basic mine valuation problems on the Witwatersrand, *J. Chem. Metall. Min. Soc. S. Afr.*, *52*, 119–139.
Krige, D. G. (1966), Two-dimensional weighted moving average trend surfaces for ore evaluation, *J. S. Afr. Inst. Min. Metall.*, *66*, 13–38.
Laslett, G. M. (1994), Kriging and splines: An empirical comparison of their predictive performance in some applications, *J. Am. Stat. Assoc.*, *89*, 391–409, doi:10.2307/2290837.
Legates, D. R., and G. J. McCabe (1999), Evaluating the use of "goodness-of-fit" measures in hydrologic and hydroclimatic model validation, *Water Resour. Res.*, *35*, 233–241, doi:10.1029/1998WR900018.
Maraun, D., T. J. Osborn, and H. W. Rust (2012), The influence of synoptic airflow on UK daily precipitation extremes. Part II: Regional climate model and E-OBS data validation, *Clim. Dyn.*, *39*, 287–301, doi:10.1007/s00382-011-1176-0.

Matheron, G. (1963), Principles of geostatistics, *Econ. Geol.*, *58*, 1246–1266.
Michaelides, S. C., K. Savvidou, K. A. Nicolaides, A. Orphanou, G. Photiou, and C. Kannaouros (2008), Synoptic, thermodynamic and agroeconomic aspects of severe hail events in Cyprus, *Nat. Hazard. Earth Syst. Sci.*, *8*, 461–471, doi:10.5194/nhess-8-461-2008.
Michaelides, S. C., F. S. Tymvios, and T. Michaelidou (2009), Spatial and temporal characteristics of the annual rainfall frequency distribution in Cyprus, *Atmos. Res.*, *94*, 606–615, doi:10.1016/j.atmosres.2009.04.008.
Murphy, A. H., and E. S. Epstein (1989), Skill scores and correlation coefficients in model verification, *Mon. Weather Rev.*, *117*, 572–581, doi:10.1175/1520-0493(1989)117<0572:SSACCI>2.0.CO;2.
Ninyerola, M., X. Pons, and J. M. Roure (2000), A methodological approach of climatological modelling of air temperature and precipitation through GIS techniques, *Int. J. Climatol.*, *20*, 1823–1841, doi:10.1002/1097-0088(20001130)20:14<1823::AID-JOC566>3.0.CO;2-B.
Nychka, D., et al. (2006), *Fields: Tools for Spatial Data*, National Center for Atmospheric Research, Boulder, CO, http://www.cgd.ucar.edu/Software/Fields.
Parkes, B. L., F. Wetterhall, F. Pappenberger, Y. He, B. D. Malamud, and H. L. Cloke (2013), Assessment of a 1-hour gridded precipitation dataset to drive a hydrological model: A case study of the summer 2007 floods in the Upper Severn, UK, *Hydrol. Res.*, *44*, 89–105, doi:10.2166/nh.2011.025.
Pashiardis, S. (2009), Development of intensity duration frequency curves, Series of Meteorological Notes No. 15, Cyprus Meteorological Service, Nicosia, Cyprus, 106 pp., (In Greek).
Pebesma, E. J. (2004), Multivariable geostatistics in S: The gstat package, *Comput. Geosci.*, *30*, 683–691, doi:10.1016/j.cargo.2004.03.012.
Perry, M., and D. Hollis (2005), The generation of monthly gridded datasets for a range of climate variables over the UK, *Int. J. Climatol.*, *25*, 1041–1054, doi:10.1002/joc.1161.
Perry, M., D. Hollis, and M. Elms (2009), The generation of daily gridded datasets of temperature and rainfall for the UK, Clim. Memo., 24, UK Met Off., Exeter, U. K.
Rubel, F., K. Brugger, P. Skomorowski, and M. Kottek (2004), Daily and 3-hourly Quantitative Precipitation Estimates for ELDAS, p. 32, Biometeorology Group, Univ. Vet. Med., Vienna, paper presented at the ECMWF/ELDAS workshop on Land Surface Assimilation, ECMWF, Reading, 8– 11 November.
Rupp, A. J., B. A. Bailey, S. S. P. Shen, C. K. Lee, and B. S. Strachan (2010), An error analysis for the hybrid gridding of Texas daily precipitation data, *Int. J. Climatol.*, *30*, 601–611, doi:10.1002/joc.1917.
Schmidli, J., C. Frei, and C. Schar (2001), Reconstruction of mesoscale precipitation fields from sparse observations in complex terrain, *J. Clim.*, *14*, 3289–3306, doi:10.1175/1520-0442(2001)014<3289:ROMPFF>2.0.CO;2.
Shen, S. S. P., P. Dzikowski, L. Guilon, and D. Griffith (2001), Interpolation of 1961–97 daily temperature and precipitation data onto Alberta polygons of ecodistrict and soil landscapes of Canada, *J. Appl. Meteorol.*, *40*, 2162–2177, doi:10.1175/1520-0450(2001)040<2162:IODTAP>2.0.CO;2.
Shepard, D. S. (1968), A two-dimensional interpolation function for irregularly-spaced data, Proceedings of the 1968 ACM National Conference, pp. 517–524, doi:10.1145/800186.810616.
Shepard, D. S. (1984), *Computer Mapping: The SYMAP Interpolation Algorithm*, pp. 133–145, Springer, New York.
Supit, I., C. A. van Diepen, A. J. W. de Wit, J. Wolf, P. Kabat, B. Baruth, and F. Ludwig (2012), Assessing climate change effects on European crop yields using the Crop Growth Monitoring System and a weather generator, *Agric. For. Meteorol.*, *164*, 96–111, doi:10.1016/j.agrformet.2012.05.005.
Symeonakis, E., R. Bonifacio, and N. Drake (2009), A comparison of rainfall estimation techniques for sub-Saharan Africa, *Int. J. Appl. Earth Obs. Geoinf.*, *11*, 15–26, doi:10.1016/j.jag.2008.04.002.
Szymanowski, M., and M. Kryza (2012), Geographically weighted regression – Kriging method for spatial interpolation of air temperature in Poland, EMS Annual Meeting Abstracts, 9, EMS2012-300.
Vicente-Serrano, S. M., S. Sanchez, and J. M. Cuadrat (2003), Comparative analysis of interpolation methods in the middle Ebro Valley (Spain): Application to annual precipitation and temperature, *Clim. Res.*, *24*, 161–180, doi:10.3354/cr024161.
Wahba, G., and J. Wendelberger (1980), Some new mathematical methods for variational objective analysis using splines and cross validation, *Mon. Weather Rev.*, *108*, 1122–1143, doi:10.1175/1520-0493(1980)108<1122:SNMMFV>2.0.CO;2.
Wang, X. L., and Y. Feng (2010), RHtestsV3 User Manual. [Available at http://cccma.seos.uvic.ca/ETCCDMI/software.shtml.]
Wang, X. L., H. Chen, Y. Wu, Y. Feng, and Q. Pu (2010), New techniques for detection and adjustment of shifts in daily precipitation data series, *J. Appl. Meteorol. Climatol.*, *49*, 2416–2436, doi:10.1175/2010JAMC2376.1.
Weber, D., and E. Englund (1992), Evaluation and comparison of spatial interpolators, *Math. Geol.*, *24*, 381–391, doi:10.1007/BF00891270.
Wilks, D. S. (2006), *Statistical Methods in Atmospherical Sciences*, 2nd ed., pp. 627, Elsevier, New York.
Willmott, C. J., C. M. Rowe, and W. D. Philpot (1985), Smallscale climate maps: A sensitivity analysis of some common assumptions associated with grid-point interpolation and contouring, *Am. Cartogr.*, *12*, 5–16.
Yatagay, A., K. Kamiguchi, O. Arakawa, A. Hamada, N. Yasutomi, and A. Kitoh (2012), APHRODITE constructing a long-term daily gridded precipitation dataset for Asia based on a dense network of rain gauges, *Bull. Am. Meteorol. Soc.*, *93*, 1401–1415, doi:10.1175/BAMS-D-11-00122.1.